Chem Rev Lett 5 (2022) 113-118

Research Article

Journal of Chemistry Letters
journal homepage: www.chemrevlett.com
ISSN (online): 2645-4947 (print) 2676-7279

Inhibiting effect of a synthesized organic compound, [3-(4-methoxyphenyl)isoxazole-5-yl]-methanol, on copper in 1 M sulfuric acid solution

Adibe Khezri[1], Ladan Ejlali[1], Moosa Eshaghi[*1], Mohammad Taghi Vardini[1], Hadi Basharnavaz[2]

[1]*Department of Chemistry, Tabriz Branch, Islamic Azad University, Tabriz, Iran*
[2]*Department of Chemistry, Faculty of Science, University of Mohaghegh Ardabili, Ardabil, Iran*

ARTICLE INFO

Article history:
Received
Received in revised form
Accepted
Available online

Keywords:
Copper;
Corrosion;
Organic inhibitor
EIS
Potentiodynamic polarization

ABSTRACT

[3-(4-Methoxyphenyl)isoxazole-5-yl]-methanol was synthesized and used as an efficient inhibitor to protect copper in 1 M sulfuric acid solution. Corrosion studies were performed by electrochemical techniques, including electrochemical impedance spectroscopy (EIS) and potentiodynamic polarization (PDP), and quantum chemical calculations. The effect of temperature on the copper corrosion and inhibitor performance was also investigated. The data obtained from the analysis of the polarization curves disclosed that the corrosion current density (Icorr) of the metal dissolution decreased in the presence of inhibitor. This may indicate a reduction in the corrosion rate, resulting from the adsorption of inhibitor molecules on the active sites of the copper surface. Such a result was confirmed by the measured Nyquist diagrams, where total resistance increased with the addition of inhibitor to the medium. It was also found that the inhibitor adsorption on the copper surface obeyed from the Langmuir isotherm, and the adsorption process occurred both physically and chemically.

1. Introduction

Due to its high mechanical, electrical, and thermal features, copper is one of the most widely used metals in human life and various industrial fields. However, oxidation in the air causes a relatively dense oxide film, whose main components are CuO and $Cu(OH)_2$, on the copper surface. As a result, the thermal and electrical conductivities of copper may be adversely affected so that the applications of the copper products will be significantly limited. Accordingly, pickling as an efficient pretreatment is commonly used to remove the oxide film from the copper surface to reach a bright surface. This operation increases the possibility of corrosion for copper, making the use of metal corrosion inhibitors in the pickling bath necessary. Effective corrosion inhibitors are organic compounds because of having conjugated double bonds, heteroatoms, and polar functional groups, which can serve as active sites to adsorb on the metal surface [1–4].

However, many of such corrosion inhibitors are restricted in their applications because of serious problems that they impose on the environment. Accordingly, the environmental regulations proposed applying compounds that are not harmful to the environment to prevent the corrosion of industrial metallic facilities.

In recent years, many efforts have been made to explore low-toxic and non-toxic efficient corrosion inhibitors [5–9]. Within this framework, drugs or drug-like compounds have attracted much attention for use as inhibitors [10–13].

Components containing the isoxazole ring are an essential class of drugs, which could be an appropriate candidate for inhibition purposes. The O and N atoms existing on the isoxazole ring give the possibility of strong adsorption on the metal surface. On this basis, the present work aims to study the inhibiting effect of a synthesized isoxazole compound named [3-(4-methoxyphenyl)isoxazole-5-yl]-methanol on the copper corrosion in sulfuric acid solution.

2. Experimental

2.1. Synthesis of [3-(4-methoxyphenyl)isoxazole-5-yl]-methanol

In a 500 ml double-walled balloon, 11.75 mmol (87

∗ Corresponding author. e-mail: eshaghi.m@iaut.ac.ir

ml) of 4-methoxybenzaldoxime, 175 mmol (10 ml) of propargyl alcohol, and 50 ml of dichloromethane were mixed with the help of a magnetic stirrer. Then, 120 ml of 5.5% sodium hypochlorite was added dropwise, and the reaction mixture was stirred at room temperature for 48 h.

After completion of this time, the balloon's contents were poured into a 250 ml separating funnel, and the organic phase was separated from the aqueous phase. The separated organic phase was dried by sodium sulfate, and after filtration and extraction of the solvent, the pure substance was obtained as a brown solid at the amount of 52.12 g (92% yield) and a melting point of 57 °C.

2.2. Electrochemical experiments

Copper specimens with a size of 1×1 cm were cut from the sheet and abraded with a series of emery papers and then washed with double-distilled water, degreased with acetone, and dried in air. Electrochemical corrosion experiments were performed in a standard three-electrode cell consisting of a platinum wire, a mounted copper coupon, and a calomel electrode as the counter, working, and reference electrodes, respectively.

Electrochemical impedance spectroscopy (EIS) measurements were carried out using Autolab PGSTAT30 Potentiostat-Galvanostat at open circuit potential (OCP), stable during the EIS measurement, in a frequency range of 100 kHz–10 mHz. Potentiodynamic polarization was measured in a potential range of −250 to 250 mV versus the OCP at the scan rate of 2 mV s^{-1}. The immersion time before each measurement was about 30 min. The obtained experimental EIS and PDP data were analyzed using the software Zview2 and Nova, respectively.

3. Results and Discussion

3.1. Characterization spectra

The FT-IR spectrum of the synthesized inhibitor is shown in Fig. S1 (Supporting Information).

According to this figure, the absorption band that appeared in the range of 3220-3500 cm-1 was attributed to the O-H stretching vibration. The band in the region between 3010 and 3120 cm-1 was related to the stretching vibrations of aromatic C-H bonds. The bands observed in the range of 2940-2820 cm-1 were related to the symmetric and asymmetric stretching vibrations of the aliphatic C-H bonds.

The stretching vibrations of the rings were observed at 1600, 1570, 1470, and 1430 cm-1, and the stretching vibration of C=N of the isoxazole ring was monitored at 1620 cm-1.

The N-O stretching vibration of the aromatic ring created an absorption band in the range of 1600-840 cm-1. The absorption band at 1170 cm-1 was also described by the stretching vibration of the O-C bond. The absorption bands of the aromatic rings were found in the range of 1600-1475 cm-1. Furthermore, two strong bands were observed in the region from 1040 to 1250 cm-1, belonging to the methoxy group attached to the phenyl ring.

The 1H NMR spectrum of the prepared inhibitor is depicted in Fig. S2. From this figure, it was concluded that the singlet peak at 6.2 ppm corresponded to the resonance of the alcoholic proton. The singlet observed at 3.85 ppm was related to the protons of the methoxy group, and the singlet appeared at 4.49 ppm was attributed to two protons of the methylene group. The singlet observed at 6.5 ppm corresponded to the proton of the isoxazole ring. The doublet peak observed at 6.98 ppm was related to two protons of the phenyl ring in the ortho position. A doublet was also observed at 7.7 ppm, corresponding to two protons of the phenyl ring in the meta position. Finally, the singlet peak that appeared at 7.2 ppm was related to the solvent proton.

The 13C NMR spectrum of the inhibitor is illustrated in Fig. S3. According to the spectrum, the peaks observed at 54.18 and 55.12 ppm belonged to the carbons of the methoxy and methylene groups, respectively. The peak found from 75.67 to 76.31 ppm was attributed to the CDCl3 solvent, and the peak observed at 98.7 ppm was related to the hydrogen-bonded carbon of the isoxazole ring. The two overlapped peaks that appeared at 113 and 113.2 ppm corresponded to the two carbons of the phenyl ring in the ortho position. The peak at 120 ppm was related to the phenyl carbon by which the phenyl ring connects to the isoxazole ring.

The two overlapped peaks observed at 127 and 127.3 ppm were attributed to the two carbons of the phenyl ring in the meta position. The peaks at 159.89 and 160.93 ppm were related to the isoxazole carbons by which the isoxazole ring connects to the phenyl ring and methylene group, respectively. Finally, the peak at 171 ppm was related to the phenyl carbon by which the phenyl ring connects to the methylene group.

3.2. Potentiodynamic polarization

The potentiodynamic polarization plots obtained for copper in 1 M sulfuric acid solution without and with various concentrations of the inhibitor at temperatures ranging from 25 to 70 oC are shown in Fig. 1. The relevant kinetic parameters, including Tafel slopes (ba and bc), polarization resistance (RP), and corrosion current density (Icorr) estimated through extrapolation of the linear segments of the curves, are given in Table 1. The data included in this table indicated that at all the studied temperatures, the Icorr values of copper in the inhibited solutions were lower than those in the blank solution. The smaller values of Icorr in the inhibitor-containing solutions were evidence of a decrease in the corrosive attack of the copper surface, resulting from the adsorption of inhibitor molecules on the metal surface. It was also found that the decreasing trend observed in Icorr was dependent on the inhibitor concentration so that an

increase in the amount of inhibitor led to a reduction in the Icorr values.

Table 1. Potentiodynamic polarization parameters obtained for copper in 1 M sulfuric acid solution in the absence and presence of various concentrations of inhibitor at temperatures ranging from 25 to 70 ºC

T()	*C(ppm)*	**-Ecorr(mV/SCE)**	*Icorr(µA cm-2)*	*Rp(Ω)*	*bc(V dec-1)*	*ba(V dec-1)*	η(%)
25	25	390.3	2.02	1591.3	0.05550	0.11376	78.78
	50	392.7	1.79	1593.5	0.05142	0.10068	78.81
	100	401.2	1.68	1954.9	0.06818	0.11152	82.73
	300	403.2	1.49	1963.6	0.07040	0.12759	82.80
	600	407.5	1.15	2569.2	0.06620	0.09669	86.85
	Blank	387.1	18.25	337.6	0.06486	0.06265	-
40	25	326.5	3.13	1383.0	0.06081	0.12739	78.20
	50	353.3	2.60	1744.8	0.04794	0.08599	82.72
	100	381.4	2.45	1802.0	0.04982	0.09949	83.27
	300	374.1	2.21	1961.0	0.04870	0.07840	84.63
	600	376.1	2.09	2282.8	0.04074	0.08427	86.79
	Blank	313.1	20.80	301.4	0.04834	0.08135	-
50	25	376.6	3.92	299.1	0.06263	0.06949	74.36
	50	369.3	3.87	300.1	0.04197	0.06665	74.42
	100	381.5	3.68	1043.2	0.04285	0.09945	75.45
	300	383.9	3.32	1608.2	0.05671	0.11490	84.07
	600	391.2	2.98	1878.3	0.06109	0.07586	86.36
	Blank	368.3	23.10	256.1	0.02678	0.05351	-
70	25	364.4	4.97	179.1	0.07448	0.10236	76.42
	50	376.6	4.89	228.3	0.06058	0.06209	42.01
	100	391.2	4.76	473.7	0.04202	0.06068	72.04
	300	393.7	4.35	479.2	0.06628	0.09080	72.37
	600	396.3	3.92	502. 9	0.06172	0.08281	73.67
	Blank	369.3	29.50	132.4	0.03769	0.08223	-

Table 2. EIS parameters obtained for copper in 1 M sulfuric acid solution in the absence and presence of various concentrations of inhibitor at temperatures ranging from 25 to 70 ºC.

T (℃)	C (ppm)	CPEf Y0×10-6 (Ω-1cm-2Sn)	n	Rf (Ω cm2)	CPE-dl Y0×10-6 (Ω-1cm-2Sn)	n	Rct (Ω cm2)	Rtotal (kΩ cm2)	W (Ω cm2 s1/2)
25	Blank	352.28	0.45	1.75	0.82	0.88	250.20	251.95	321.50
	25	0.96	0.84	146.30	476.65	0.50	979.50	1125.80	--
	50	105.52	0.83	245.90	358.31	0.56	999.20	1245.10	--
	100	153.18	0.82	252.20	348.87	0.54	1153.00	1405.20	--
	300	147.74	0.79	7.37	200.69	0.57	2196.00	2203.37	--
	600	0.20	0.90	27.92	251.23	0.60	2930.00	2957.92	--
40	Blank	456.35	0.45	1.37	0.57	0.89	220.50	221.87	256.30
	25	104.76	0.82	159.00	468.85	0.52	681.30	840.30	--
	50	179.92	0.78	277.80	3954.10	0.55	741.90	1019.70	--
	100	161.11	0.76	634.10	8740.40	0.83	457.40	1091.50	--
	300	270.45	0.70	1106.00	7802.70	0.98	235.40	1341.40	--
	600	162.83	0.56	923.89	1364.70	0.98	995.9	1919.79	--
50	Blank	165.58	0.82	7.75	1525.90	0.48	211.80	219.55	97.44
	25	0.97	0.86	43.53	698.12	0.50	343.50	387.03	--
	50	0.87	0.83	51.13	491.27	0.51	608.70	659.83	--
	100	0.94	0.84	45.52	451.97	0.51	738.80	784.32	--
	300	149.29	0.76	128.00	318.45	0.51	1213.00	1341.00	--
	600	0.37	0.86	13.54	320.47	0.54	1483.00	1496.45	--
70	Blank	103.88	0.84	9.86	1227.20	0.46	201.80	211.66	174.5
	25	225.70	0.78	79.50	1441.00	0.51	315.50	395.00	--
	50	235.73	0.76	66.49	1987.70	0.50	278.20	344.69	--
	100	198.94	0.76	135.50	1113.40	0.50	470.90	606.40	--
	300	0.62	0.87	7.76	665.42	0.51	672.50	680.26	--
	600	106.62	0.77	102.80	300.56	0.51	1106.00	1208.80	--

Table 3. Values of the coefficients A, B, C, and D in Eq. (2) obtained at all the studied temperatures.

T (ºC)	*A*	*B*	*C*	*D*
25	0.9496	0.6739	1.0090	0.9881
40	0.9410	0.6186	1.0106	0.9861
50	0.9761	0.8455	1.0043	0.9944
70	1.0145	1.0935	0.9974	1.0034

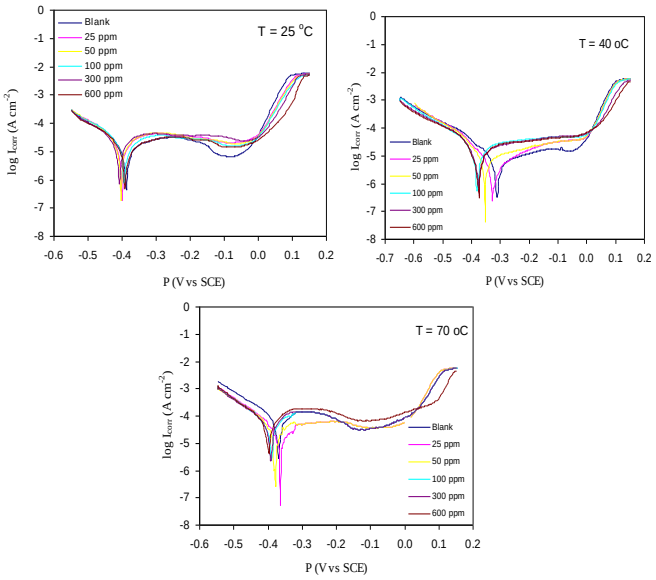

Fig. 1. Tafel curves for copper in in 1 M sulfuric acid solution in the absence and presence of various concentrations of inhibitor at temperatures ranging from 25 to 70 oC.

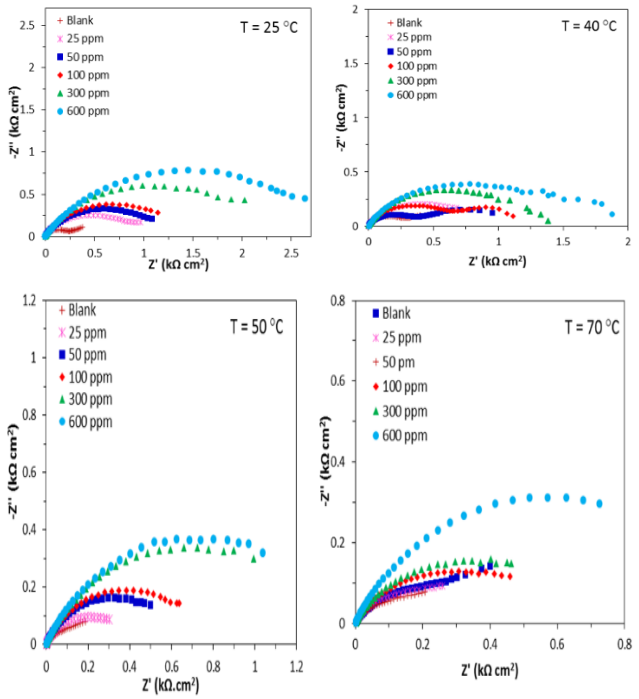

Fig. 2. Nyquist diagrams for copper in in 1 M sulfuric acid solution in the absence and presence of various concentrations of inhibitor at temperatures ranging from 25 to 70 oC.

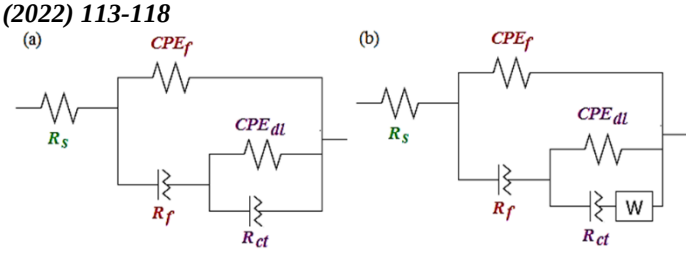

Fig. 3. Equivalent circuit models used to fit experimental EIS data. The circuits (a) and (b) were applied for the solutions with and without inhibitor, respectively.

For instance, the Icorr value of 18.25 µA cm-2 in the blank solution at 25 oC decreased to 2.02 and 1.15 µA cm-2 in the presence of 25 and 600 ppm of the inhibitor, respectively. Table 1 indicates that the presence of inhibitor in the corrosive medium shifted the corrosion potential to more negative values. Such behavior was previously reported for copper in 0.5 M sulfuric acid solution [3,4]. The displacement of Ecorr toward the cathodic direction was less than 85 mV for all cases. This observation is generally interpreted in the literature as a mixed-type inhibiting effect of the inhibitor, meaning that the proposed inhibitor mitigated the copper corrosion by reducing the rates of both cathodic and anodic reactions. The obtained Icorr values were used to estimate inhibition efficiencies by the following equation [14,15]:

$$\eta = \frac{I^0_{corr} - I_{corr}}{I^0_{corr}} \times 100 \quad (1)$$

where and denote the corrosion current densities in the absence and presence of inhibitor, respectively. According to Table 1, the inhibition efficiency increased with increasing the inhibitor concentration and reached a maximum value of 86.85% in the presence of 600 ppm of the inhibitor at 25 oC. It was also observed that the inhibition efficiency at the optimum concentration of 600 remained almost constant with increasing temperature from 25 to 50 oC, but then experienced a relatively large reduction at 70 oC. This behavior demonstrated that the proposed inhibitor could be used effectively in a specific temperature range without any diminishing in its performance.

3.3. EIS results

EIS measurements were performed in the absence and presence of various inhibitor concentrations in 1 M H2SO4 solution. Fig. 2 illustrates the Nyquist diagrams of the inhibited and uninhibited copper samples immersed in the aggressive solution at 25, 40, 50, and 70 ℃. The Nyquist plots of the blank solution depicted two capacitive time constants at higher and medium frequencies and a straight line at low frequency, which is related to the Warburg impedance.

Warburg is attributed The equivalent circuit models shown in Fig. 3 were applied to fit the experimental EIS data. The parameters obtained from fitting are given in Table 2. The solution resistance is Rs, the resistance of

inhibitor film formed on the copper surface is Rf, the charge transfer resistance is Rct, and the Warburg impedance is W. CPEdl and CPEf are constant phase elements corresponding to the film and double layer capacitance, respectively. The impedance of CPE is calculated by the equation: $Z_{CPE} = (Y_0 j\omega)^{-n}$, where Y_0, j, ω, and n are the admittance of CPE, imaginary root, angular frequency, and CPE exponent, respectively. Table 2 indicated that at a constant temperature, increasing the inhibitor concentration from 25 to 600 ppm resulted in an improvement in the Rct and Rtotal values. On this basis, it could be concluded that the charge transfer process was retarded by forming a film of inhibitor on the copper surface. On the other hand, increasing temperature form 25 to 70 oC disturbed the film formation on the surface, leading to a reduction in the corrosion resistance.

3.4. Quantum chemical calculations

Density functional theory (DFT) was used to make a relationship between the molecular structure of the inhibitor and its inhibition performance. DFT calculations were performed using Gaussian03 at the level of B3LYP/6-31G** to optimize the inhibitor structure and obtain some quantum chemical parameters, such as the energy of the highest occupied molecular orbital (EHOMO), the energy of the lowest unoccupied molecular orbital (ELUMO), and dipole moment (μ). The calculated values of these parameters were obtained as EHOMO = -0.23587 eV, ELUMO = -0.03646 eV, and μ = 1.3182. These parameters were connected to the inhibition efficiency through the quantum structure-activity relationship (QSAR). The following non-linear QSAR was applied to make a correlation between the experimental inhibition efficiencies and calculated quantum chemical parameters [16]:

$$\frac{\eta}{100} = \frac{(AE_{\mathrm{HOMO}} + BE_{\mathrm{LUMO}} + C\mu - D)C_{\mathrm{inh}}}{1 + (AE_{\mathrm{HOMO}} + BE_{\mathrm{LUMO}} + C\mu - D)C_{\mathrm{inh}}} \quad (2)$$

The obtained values of the coefficients *A*, *B*, *C*, and *D* at each temperature are collected in Table 3. Using these coefficients and Eq. (2), one can predict inhibition efficiencies at any desired concentration of the inhibitor.

4. Conclusions

According to the results obtained in this work, increasing the concentration of inhibitor from 25 to 600 ppm decreased the corrosion rate of copper. Such a reduction in corrosion was more effective in temperatures lower than 50 oC, where the inhibition efficiency exhibited a large decrease as the temperature was raised to 70 oC. It was also concluded that the studied inhibitor affected both anodic and cathodic reactions with a small shift of corrosion potential towards the cathodic direction. This indicated that the proposed compound acted as a mixed-type inhibitor, but predominately controlled the hydrogen evolution as the cathodic reaction.

Acknowledgments

The authors wish to thank the Islamic Azad University, Tabriz Branch for financial support of the present work.

References

[1] Z. Gong, S. Peng, X. Huang, L. Gao, Investigation the corrosion inhibition effect of itraconazole on copper in H_2SO_4 at different temperatures: Combining experimental and theoretical studies, Materials (Basel). 11 (2018) 2107.

[2] A. Jmiai, B. El Ibrahimi, A. Tara, M. Chadili, S. El Issami, O. Jbara, A. Khallaayoun, L. Bazzi, Application of Zizyphus Lotuse-pulp of Jujube extract as green and promising corrosion inhibitor for copper in acidic medium, J. Mol. Liq. 268 (2018) 102–113.

[3] J. Zhang, L. Zhang, G. Tao, A novel and high-efficiency inhibitor of 5-(4-methoxyphenyl)-3h-1, 2-dithiole-3-thione for copper corrosion inhibition in sulfuric acid at different temperatures, J. Mol. Liq. 272 (2018) 369–379.

[4] Y. Xu, S. Zhang, W. Li, L. Guo, S. Xu, L. Feng, L.H. Madkour, Experimental and theoretical investigations of some pyrazolo-pyrimidine derivatives as corrosion inhibitors on copper in sulfuric acid solution, Appl. Surf. Sci. 459 (2018) 612–620.

[5] H. Ashassi-Sorkhabi, S. Moradi-Alavian, A. Kazempour, Salt-nanoparticle systems incorporated into sol-gel coatings for corrosion protection of AZ91 magnesium alloy, Prog. Org. Coatings. 135 (2019) 475–482.

[6] H. Ashassi-Sorkhabi, A. Kazempour, Chitosan, its derivatives and composites with superior potentials for the corrosion protection of steel alloys: A comprehensive review, Carbohydr. Polym. (2020) 116110.

[7] H. Ashassi-Sorkhabi, A. Kazempour, Incorporation of organic/inorganic materials into polypyrrole matrix to reinforce its anticorrosive properties for the protection of steel alloys: A review, J. Mol. Liq. (2020) 113085.

[8] H. Ashassi-Sorkhabi, S. Moradi-Alavian, R. Jafari, A. Kaz empour, E. Asghari, Effect of amino acids and montmorillonite nanoparticles on improving the corrosion protection characteristics of hybrid sol-gel coating applied on AZ91 Mg alloy, Mater. Chem. Phys. 225 (2019) 298–308.

[9] H. Ashassi-Sorkhabi, S. Moradi-Alavian, M.D. Esrafili, A. Kazempour, Hybrid sol-gel coatings based on silanes-amino acids for corrosion protection of AZ91 magnesium alloy: Electrochemical and DFT insights, Prog. Org. Coatings. 131 (2019) 191–202.

[10] L. Zhou, S. Zhang, B. Tan, L. Feng, B. Xiang, F. Chen, W. Li, B. Xiong, T. Song, Phenothiazine drugs as novel and eco-friendly corrosion inhibitors for copper in sulfuric acid solution, J. Taiwan Inst. Chem. Eng. 113 (2020) 253–263.

[11] N. Palaniappan, J. Alphonsa, I.S. Cole, K. Balasubramanian, I.G. Bosco, Rapid investigation expiry drug green corrosion inhibitor on mild steel in NaCl medium, Mater. Sci. Eng. B. 249 (2019) 114423.

[12] M. Abdallah, E.A.M. Gad, M. Sobhi, J.H. Al-Fahemi, M.M. Alfakeer, Performance of tramadol drug as a safe inhibitor for aluminum corrosion in 1.0 M HCl solution and understanding mechanism of inhibition using DFT, Egypt. J. Pet. 28 (2019) 173–181.

[13] V.C. Anadebe, O.D. Onukwuli, F.E. Abeng, N.A. Okafor, J.O. Ezeugo, C.C. Okoye, Electrochemical-kinetics, MD-simulation and multi-input single-output (MISO) modeling using adaptive neuro-fuzzy inference system (ANFIS) prediction for dexamethasone drug as eco-friendly corrosion inhibitor for mild steel in 2 M HCl electrolyte, J. Taiwan Inst. Chem. Eng. 115 (2020) 251–265.

[14] S. Mohamadian-Kalhor, L. Edjlali, H. Basharnavaz, M. Es'haghi, Aluminum Fumarate Metal–Organic Framework: Synthesis, Characterization, and Application as a Novel Inhibitor against Corrosion of AM60B Magnesium Alloy in Ethylene Glycol Solution, J. Mater. Eng. Perform. (2021) 1–7.

[15] R. Sadeghzadeh, L. Ejlali, M. Eshaghi, H. Basharnavaz, K. Seyyedi, Corrosion inhibition of mild steel surface by isoxazoles in HCl solution: Electrochemical studies, Chem. Rev. Lett. 4 (2021) 2–9.

[16] H. Ashassi-Sorkhabi, A. Kazempour, Z. Frouzat, Superior potentials of hydrazone Schiff bases for efficient corrosion protection of mild steel in 1.0 M HCl, J. Adhes. Sci. Technol. 35 (2021) 164–184.